Jyväskylä Summer School

Multiwave Imaging

Gunther Uhlmann

University of Washington
& University of Helsinki

Jyväskylä, Finland, August 19-23, 2013

Inverse Boundary Problems

Can one determine the internal properties of a medium by making measurements outside the medium (non-invasive)?

X-ray tomography (CAT-scans)

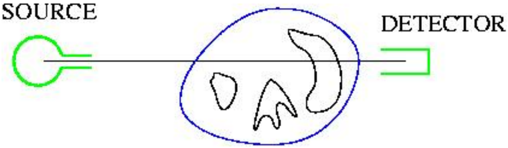

Problem: Can we recover the density from attenuation of X-rays?

X-ray Tomography

Problem: Can we recover the density from attenuation of X-rays?

Radon solved the problem in 1917

Determine the integral of density over lines

Johann Radon

Nobel Prize in Medicine (1979)

A. Cormack

G. Hounfield

Radon (1917) $n = 2$

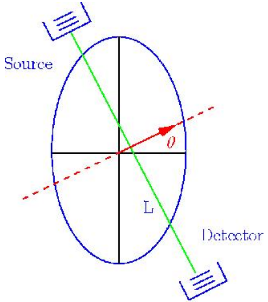

$$f(x) = \text{Unknown function}$$

$$I_{detector} = e^{-\int_L f} I_{source}$$

$$Rf(s,\theta) = g(s,\theta) = \int_{\langle x,\theta\rangle = s} f(x)dH = \int_L f$$

$$\boxed{f(x) = \frac{1}{4\pi^2}\ p.v. \int_{S^1} d\theta \int \frac{\frac{d}{ds} g(s,\theta) ds}{\langle x,\theta\rangle - s}}$$

LINEAR (No Scattering)

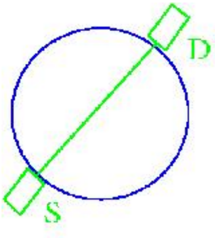

X-ray tomography (CT)

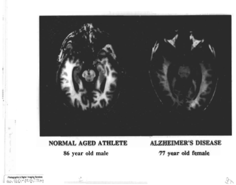

PET

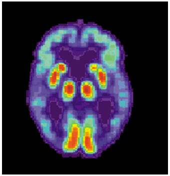

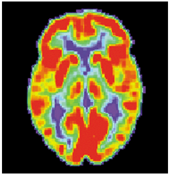

MRI

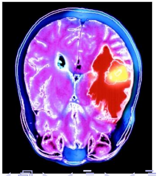

NONLINEAR (Scattering)

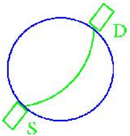

Ultrasound

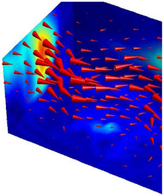

Electrical Impedance Tomography **(EIT)**

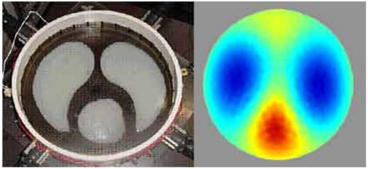

Superposition of 2 images each obtained with a single wave

One single wave is sensitive only to a given Contrast :

Ultrasound to bulk compressibility ,
Optical wave to dielectric permitivity and optical absorption,
Sonic Shear wave to shear modulus, viscosity
LF Electromagnetic wave to electrical impedance, conductivity
X ray to density
Gamma ray to radio tracer distribution
...

Spatial Resolution depends on wave physics laws and on sensor technology.

A difficult problem for radiologists: breast cancer detection

Ultrasound images of different breast lesions

benign

Fibrotic Lesion

Malign

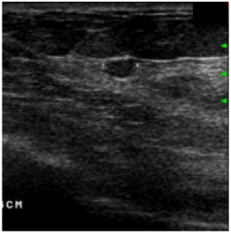

Carcinoma Grade II

benign

Viscous cyst

Good sensitivity but bad specificity

How to play Multiwave Imaging ?

Three potential Interactions between different waves

- *The interaction of the first wave with tissues* can generate *a second kind of wave*

PhotoAcoustic Imaging
ThermoAcoustic Imaging

- *The first wave* ***IS TAGGED*** *locally by a second kind of wave*

AcoustoOptical Imaging
Electrical Impedance Imaging with Ultrasound

- *A first wave travelling much faster than the second one can be used to produce* a movie *of the slow wave propagation*

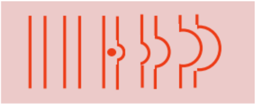

Transient Elastography
Shear Wave imaging (Supersonic mode)

A unique case that allows the observation of the near field of the slow wave inside the body ,

Photoacoustic Effect: The sound of light

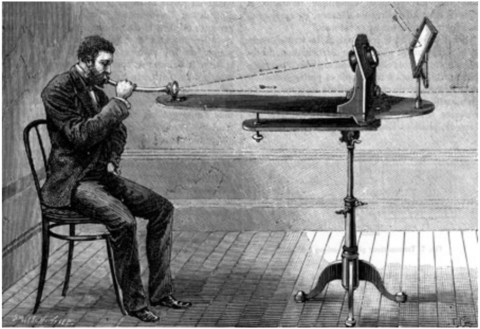

Picture from Economist (The sound of light)

Graham Bell: When rapid pulses of light are incident on a sample of matter they can be absorbed and the resulting energy will then be radiated as heat. This heat causes detectable sound waves due to pressure variation in the surrounding medium.

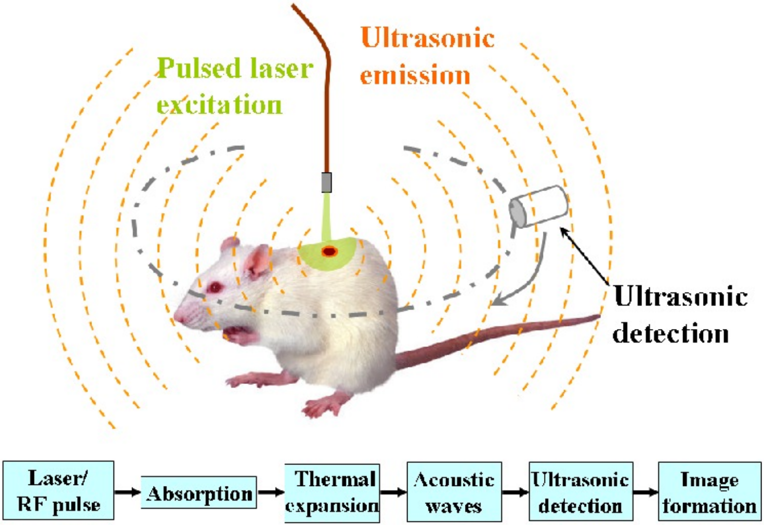
Pulsed laser excitation
Ultrasonic emission
Ultrasonic detection
Laser/ RF pulse
Absorption
Thermal expansion
Acoustic waves
Ultrasonic detection
Image formation

Wikipedia

(Loading Melanoma3DMovie.avi)

Mathematical Model

First Step: in PAT and TAT is to reconstruct $H(x)$ from $u(x,t)|_{\partial\Omega\times(0,T)}$, where u solves

$$\boxed{\begin{aligned} (\partial_t^2 - c^2(x)\Delta)u &= 0 \quad \text{on } \mathbb{R}^n \times \mathbb{R}^+ \\ u|_{t=0} &= \beta H(x) \\ \partial_t u|_{t=0} &= 0 \end{aligned}}$$

Second Step: in PAT and TAT is to reconstruct the optical or electrical properties from $H(x)$ (internal measurements).

First Step:

IP for Wave Equation

$\boxed{c(x) > 0}$: acoustic speed

$$\boxed{\begin{cases} (\partial_t^2 - c^2\Delta)u &= 0 \quad \text{in } (0,T)\times\mathbb{R}^n, \\ u|_{t=0} &= f, \\ \partial_t u|_{t=0} &= 0. \end{cases}}$$

$\boxed{f}$: supported in $\bar{\Omega}$. $\boxed{\text{Measurements}}$:

$$\boxed{\Lambda f := u|_{[0,T]\times\partial\Omega}}.$$

The problem is to reconstruct the unknown f from Λf.

Prior results

Constant Speed

Kruger; Agranovsky, Ambartsoumian, Finch, Georgieva-Hristova, Jin, Haltmeier, Kuchment, Nguyen, Patch, Quinto, Rakesh, Wang, Xu . . .

Variable Speed (Numerical Results)

Anastasio et. al., Burgholzer, Cox et. al., Georgieva-Hristova, Grun, Haltmeir, Hofer, Kuchment, Nguyen, Paltauff, Wang, Xu...
(Time reversal)

Partial Data

Problem is uniqueness, stability and reconstruction with measurements on a part of the boundary. There were no results so far for the variable coefficient case, and there is a uniqueness result in the constant coefficients one by Finch, Patch and Rakesh (2004).

Ω=ball, constant speed

$\boxed{c = 1}$, $\boxed{\Omega}$: unit ball, $\boxed{n = 3}$. Explicit Reconstruction Formulas (Finch, Haltmeier, Kunyansky, Nguyen, Patch, Rakesh, Xu, Wang).

$\boxed{g(x,t) = \Lambda f}$, $x \in S^{n-1}$. In 3D,

$$\boxed{f(x) = -\frac{1}{8\pi^2}\Delta_x \int_{|y|=1} \frac{g(y,|x-y|)}{|x-y|}\,\mathrm{d}S_y.}$$

$$\boxed{f(x) = -\frac{1}{8\pi^2}\int_{|y|=1} \left(\frac{1}{t}\frac{d^2}{dt^2}g(y,t)\right)\Bigg|_{t=|y-x|}\mathrm{d}S_y.}$$

$$\boxed{f(x) = \frac{1}{8\pi^2}\nabla_x \cdot \int_{|y|=1} \left(\nu(y)\frac{1}{t}\frac{d}{dt}\frac{g(y,t)}{t}\right)\Bigg|_{t=|y-x|}\mathrm{d}S_y.}$$

The latter is a partial case of an explicit formula in any dimension (Kunyansky).

$\boxed{T = \infty}$: a backward Cauchy problem with zero initial data.
$\boxed{T < \infty}$: time reversal

$$\boxed{\begin{cases} (\partial_t^2 - c^2\Delta)v_0 &= 0 \quad \text{in } (0, T) \times \Omega, \\ v_0\big|_{[0,T]\times\partial\Omega} &= \chi h, \\ v_0\big|_{t=T} &= 0, \\ \partial_t v_0\big|_{t=T} &= 0, \end{cases}}$$

where $\boxed{h = \Lambda f}$; $\boxed{\chi}$: cuts off smoothly near $t = T$.

Time Reversal

$$f \approx A_0 h := v_0(0, \cdot) \quad \text{in } \bar{\Omega}, \text{ where } h = \Lambda f.$$

Uniqueness

Underlying metric: $\boxed{c^{-2}\mathrm{d}x^2}$. Set

$$\boxed{T_0 = \max_{x\in\bar{\Omega}} \mathrm{dist}(x, \partial\Omega).}$$

Theorem (Stefanov–U, IP 2009)

$T \geq T_0 \implies$ uniqueness. $T < T_0 \implies$ no uniqueness. We can recover $f(x)$ for $\mathrm{dist}(x, \partial\Omega) \leq T$ and nothing else.

The proof is based on the unique continuation theorem by Tataru.

Stability

$\boxed{T_1 \le \infty}$: length of the longest (maximal) geodesic through $\bar{\Omega}$.

The $\boxed{\text{“stability time”}}$: $\boxed{T_1/2}$. If $T_1 = \infty$, we say that the speed is **trapping** in Ω.

Theorem (Stefanov–U)

$T > T_1/2 \quad \Longrightarrow \quad$ *stability.*
$T < T_1/2 \quad \Longrightarrow \quad$ *no stability, in any Sobolev norms.*

The second part follows from the fact that Λ is a smoothing FIO on an open conic subset of $T^*\Omega$. In particular, if the speed is trapping, there is no stability, whatever T.

Reconstruction. Modified time reversal

A modified time reversal, harmonic extension

Given h (that eventually will be replaced by Λf), solve

$$\boxed{\left\{\begin{array}{rcl} (\partial_t^2 - c^2\Delta)v & = & 0 \quad \text{in } (0,T)\times\Omega, \\ v\big|_{[0,T]\times\partial\Omega} & = & h, \\ v\big|_{t=T} & = & \phi, \\ \partial_t v\big|_{t=T} & = & 0, \end{array}\right.}$$

where ϕ is the harmonic extension of $h(T,\cdot)$:

$$\boxed{\Delta\phi = 0, \quad \phi|_{\partial\Omega} = h(T,\cdot).}$$

Note that the initial data at $t = T$ satisfies compatibility conditions of first order (no jump at $\{T\}\times\partial\Omega$). Then we define the following pseudo-inverse

$$\boxed{Ah := v(0,\cdot) \quad \text{in } \bar{\Omega}.}$$

We are missing the Cauchy data at $t = T$; the only thing we know there is its value on $\partial\Omega$. The time reversal methods just replace it by zero. We replace it by that data (namely, by $(\phi, 0)$), having the same trace on the boundary, that minimizes the energy.

Given $U \subset \mathbb{R}^n$, the energy in U is given by

$$E_U(t,u) = \int_U \left(|\nabla u|^2 + c^{-2}|u_t|^2\right) \mathrm{d}x.$$

We define the space $H_D(U)$ to be the completion of $C_0^\infty(U)$ under the Dirichlet norm

$$\|f\|_{H_D}^2 = \int_U |\nabla u|^2 \, \mathrm{d}x.$$

The norms in $H_D(\Omega)$ and $H^1(\Omega)$ are equivalent, so

$$H_D(\Omega) \cong H_0^1(\Omega).$$

The energy norm of a pair $[f, g]$ is given by

$$\|[f,g]\|_{\mathcal{H}(\Omega)}^2 = \|f\|_{H_D(\Omega)}^2 + \|g\|_{L^2(\Omega, c^{-2}\mathrm{d}x)}^2$$

$$\boxed{A\Lambda f = f - Kf}$$

$$Kf = w(0,.)$$

where w solves

$$\begin{cases} \left(\partial_t^2 - c^2(x)\,\Delta\right) w = 0 & \text{in } (0,T)\times\Omega, \\ w\,\Big|_{[0,T]\times\partial\Omega} = 0, & \\ w\,\Big|_{t=T} = u\,\Big|_{t=T} - \phi, & \\ w_t\,\Big|_{t=T} = u_t\,\Big|_{t=T}, & \end{cases}$$

where u solves

$$\begin{cases} (\partial_t^2 - c^2\Delta)u & = & 0 & \text{in } (0,T)\times\mathbb{R}^n, \\ u\big|_{t=0} & = & f, & \\ \partial_t u\big|_{t=0} & = & 0. & \end{cases}$$

$\boxed{A\Lambda f = f - Kf}$

Consider the "error operator" K,

$$Kf = \text{first component of: } U_{\Omega,D}(-T)\Pi_\Omega U_{\mathbb{R}^n}(T)[f,0],$$

where

- $U_{\mathbb{R}^n}(t)$ is the dynamics in the whole $\mathbb{R}^n$,
- $U_{\Omega,D}(t)$ is the dynamics in Ω with Dirichlet BC,
- $\Pi_\Omega : \mathcal{H}(\mathbb{R}^n) \to \mathcal{H}(\Omega)$ is the orthogonal projection.

That projection is given by $\Pi_\Omega[f,g] = [f|_\Omega - \phi, g|_\Omega]$, where ϕ is the harmonic extension of $f|_{\partial\Omega}$.

Obviously,

$$\|Kf\|_{H_D} \leq \|f\|_{H_D}.$$

Reconstruction (whole boundary)

Theorem (Stefanov–U, IP 2009)

Let $T > T_1/2$. Then $A\Lambda = I - K$, where $\|K\|_{\mathcal{L}(H_D(\Omega))} < 1$. In particular, $I - K$ is invertible on $H_D(\Omega)$, and the inverse thermoacoustic problem has an explicit solution of the form

$$f = \sum_{m=0}^{\infty} K^m A h, \quad h := \Lambda f.$$

If $T > T_1$, then K is compact.

Reconstruction (whole boundary)

We have the following estimate on $\|K\|$:

Theorem (Stefanov–U, IP 2009)

$$\|Kf\|_{H_D(\Omega)} \leq \left(\frac{E_\Omega(u,T)}{E_\Omega(u,0)}\right)^{\frac{1}{2}} \|f\|_{H_D(\Omega)}, \quad \forall f \in H_{D(\Omega)},\ f \neq 0,$$

where u is the solution with Cauchy data $(f,0)$.

Summary: Dependence on T

(i) $T < T_0 \implies$ **no uniqueness**
Λf does not recover uniquely f. $\|K\| = 1$.

(ii) $T_0 < T < T_1/2 \implies$ **uniqueness, no stability**
We have uniqueness but not stability (there are invisible singularities). We do not know if the Neumann series converges. $\|Kf\| < \|f\|$ but $\|K\| = 1$.

(iii) $T_1/2 < T < T_1 \implies$ **stability and explicit reconstruction**
This assumes that c is non-trapping. The Neumann series converges exponentially but maybe not as fast as in the next case (K contraction but not compact). There is stability (we detect all singularities but some with 1/2 amplitude). $\|K\| < 1$

(iv) $T_1 < T \implies$ **stability and explicit reconstruction**
The Neumann series converges exponentially, K is contraction and compact (all singularities have left $\bar{\Omega}$ by time $t = T$). There is stability. $\|K\| < 1$

If c is trapping ($T_1 = \infty$), then (iii) and (iv) cannot happen.

Numerical Experiments (Qian-Stefanov-U-Zhao, SIAM J. Imaging, 2011)

Sound speed models

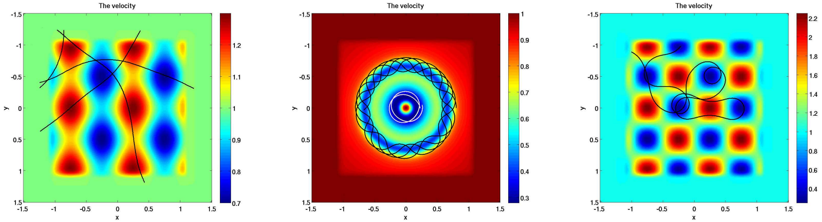

non-trapping speed c_1 radial trapping speed c_2 trapping speed c_3

Figure: Sound speed models

Shepp-Logan phantom: non-trapping c_1 (1)

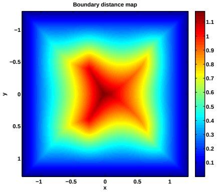

The boundary distance

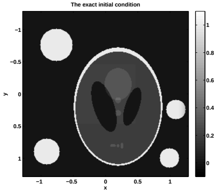

Exact

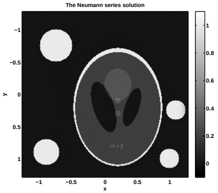

NS

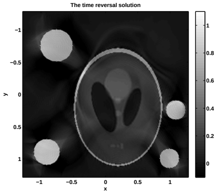

TR

Figure: Example 1, non-trapping c_1, $T = 2T_0$.

Shepp-Logan phantom: non-trapping c_1 (2)

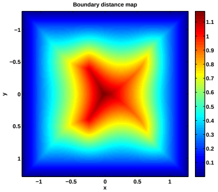

The boundary distance

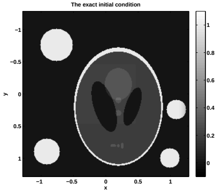

Exact

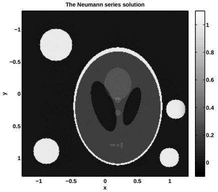

NS

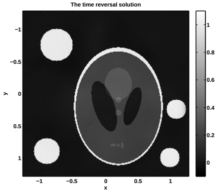

TR

Figure: Example 1, non-trapping c_1, $T = 4T_0$.

Shepp-Logan phantom: non-trapping c_1 (3)

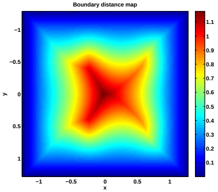

The boundary distance

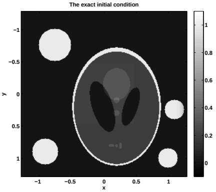

Exact

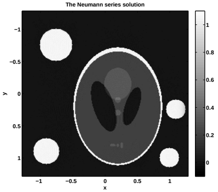

NS

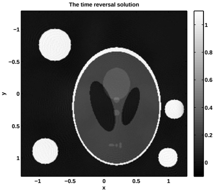

TR

Figure: Example 1, non-trapping c_1, $T = 4T_0$, with 10% noise.

Shepp-Logan phantom: trapping c_3 (4)

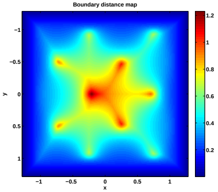

The boundary distance

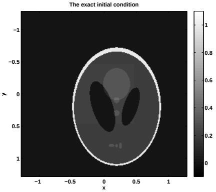

Exact

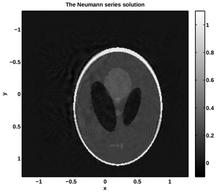

NS

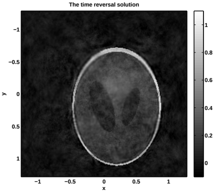

TR

Figure: Example 1, trapping c_3, $T = 4T_0$.

Zebras: non-trapping c_1 (1)

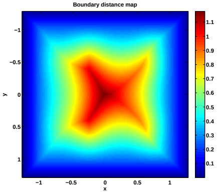

The boundary distance

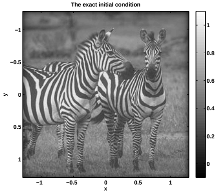

Exact

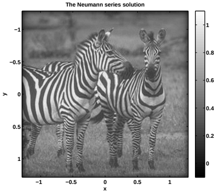

NS

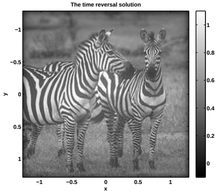

TR

Figure: Example 2, non-trapping c_1, $T = 4T_0$.

Zebras: trapping c_3 (2)

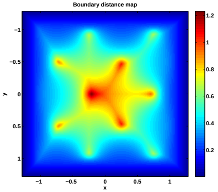

The boundary distance

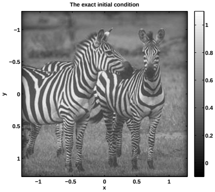

Exact

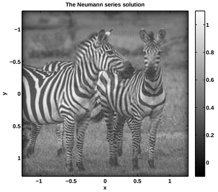

NS

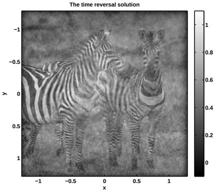

TR

Figure: Example 2, trapping c_3, $T = 4T_0$.

Zebras: radial trapping c_2 (3)

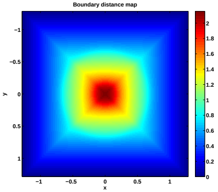

The boundary distance

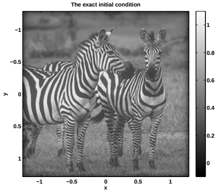

Exact

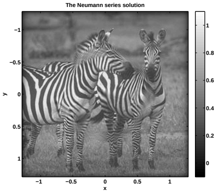

NS

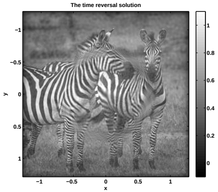

TR

Figure: Example 2, radial trapping c_2, $T = 4T_0$.

Transcranial PAT brain imaging

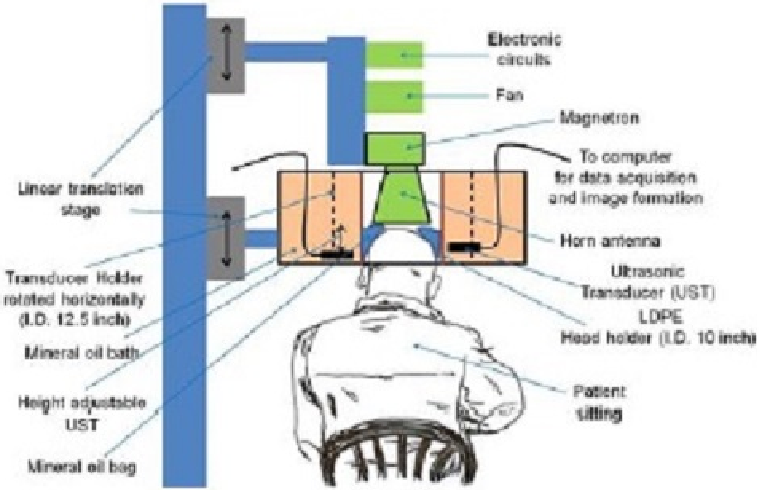

Discontinuous Speeds, Modeling Brain Imaging (Proposed by L. Wang)

Let c be piecewise smooth with a jump across a smooth closed surface Γ. The direct problem is a transmission problem, and there are reflected and refracted rays.

In brain imaging, the interface is the skull. The sound speed jumps by about a factor of 2 there. Experiments show that the ray that arrives first carries about 20% of the energy.

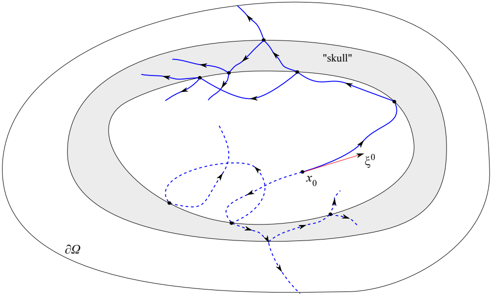

Propagation of singularities in the "skull" geometry

Propagation of singularities is the key again.
(Completely) trapped singularities are a problem, as before. Let $\mathcal{K} \subset \Omega$ be a compact set such that all rays originating from it are never tangent to Γ and non-trapping. For f satisfying

$$\operatorname{supp} f \subset \mathcal{K}$$

the Neumann series above still converges (uniformly to f).
We need a small modification to keep the support in $\mathcal{K}$ all the time. We use the projection

$$\Pi_{\mathcal{K}} : H_D(\Omega) \to H_D(\mathcal{K})$$

for that purpose.

Reconstruction

Theorem (Stefanov–U, IP 2011)

Let all rays from $\mathcal{K}$ have a path never tangent to Γ that reaches $\partial\Omega$ at time $|t| < T$. Then

$$\Pi_{\mathcal{K}} A\Lambda = I - K \text{ in } H_D(\mathcal{K}), \text{ with } \|K\|_{H_D(\mathcal{K})} < 1.$$

In particular, $I - K$ is invertible on $H_D(\mathcal{K})$, and Λ restricted to $H_D(\mathcal{K})$ has an explicit left inverse of the form

$$f = \sum_{m=0}^{\infty} K^m \Pi_{\mathcal{K}} A h, \quad h = \Lambda f.$$

The assumption $\operatorname{supp} f \subset \mathcal{K}$ means that we need to know f outside $\mathcal{K}$; then we can subtract the known part.
In the numerical experiments below, we do not restrict the support of f, and still get good reconstruction images but the invisible singularities remain invisible.

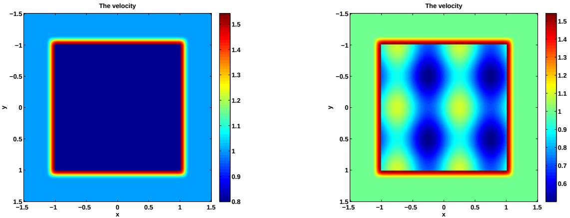

Figure: **Left**: a discontinuous piecewise sound speed c_4; **Right**: a non-piecewise constant discontinuous sound speed c_5.

Shepp-Logan phantom: discontinuous speed c_4 (1)

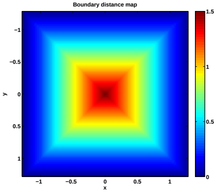

The boundary distance

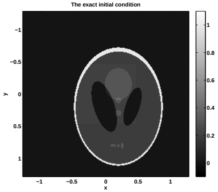

Exact

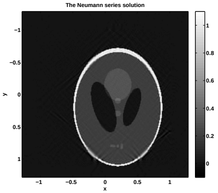

NS

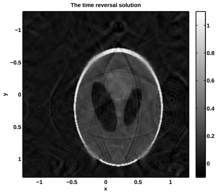

TR

Figure: Example 3, discontinuous sound speed c_4, $T = 4T_0$.

Shepp-Logan phantom: discontinuous speed c_5 (2)

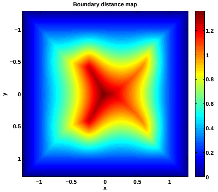

The boundary distance

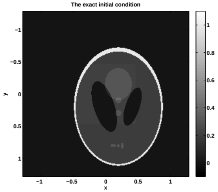

Exact

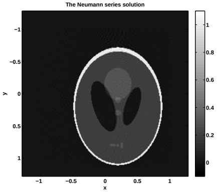

NS

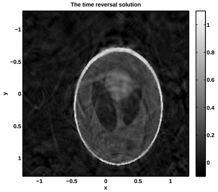

TR

Figure: Example 3, discontinuous sound speed c_5, $T = 4T_0$.

Zebras: discontinuous speed c_5

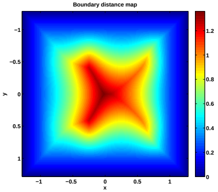

The boundary distance

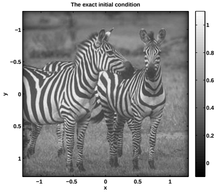

Exact

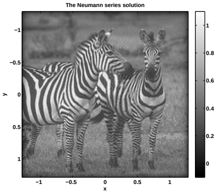

NS

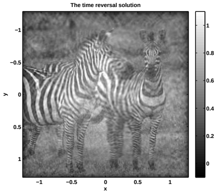

TR

Figure: Example 2, discontinuous sound speed c_5, $T = 4T_0$.

Brain imaging of square headed people

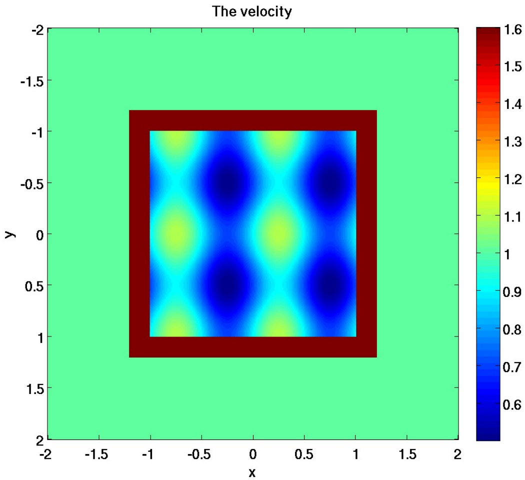

The speed jumps by a factor of 2 in average from the exterior of the "skull". The region Ω, as before, is smaller: $\Omega = [-1.28, 1.28]^2$.

A "skull" speed, Neumann series

original

$T = 2T_0$, error $= 15\%$

$T = 4T_0$, error $= 9.75\%$

$T = 8T_0$, error $= 7.55\%$

Neumann Series, 15 steps

A “skull” speed, Time Reversal

original

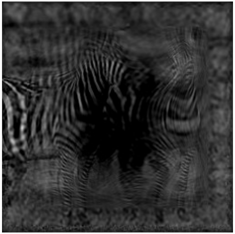

$T = 2T_0$, error $= 68\%$

$T = 4T_0$, error $= 23.7\%$

$T = 8T_0$, error $= 78.5\%$

Time Reversal. There is a lot of “white clipping” in the last image, many values in $[1, 1.6]$

A "skull" speed, Time Reversal

original

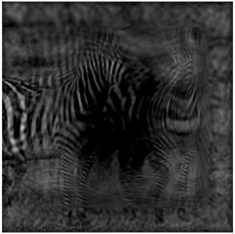

$T = 2T_0$, error $= 68\%$

$T = 4T_0$, error $= 23.7\%$

$T = 8T_0$, error $= 78.5\%$

Time Reversal. The values in last image are compressed from $[0, 1]$ to $[-0.05, 1.6]$

Original vs. Neumann Series vs. Time Reversal

original NS, error $= 7.55\%$ TR, error $= 78.5\%$

$T = 8T_0$. Original vs. Neumann Series vs. Time Reversal (the latter compressed from $[0, 1]$ to $[-0.05, 1.6]$)

Measurements on a part of the boundary

Assume that $c = 1$ outside Ω. Let $\Gamma \subset \partial\Omega$ be a relatively open subset of $\partial\Omega$. Assume now that the observations are made on $[0, T] \times \Gamma$ only, i.e., we assume we are given

$$\Lambda f|_{[0,T]\times\Gamma}.$$

We consider f's with

$$\operatorname{supp} f \subset \mathcal{K},$$

where $\mathcal{K} \subset \Omega$ is a fixed compact.

Uniqueness

Heuristic arguments for uniqueness: To recover f from Λf on $[0, T] \times \Gamma$, we must at least be able to get a signal from any point, i.e., we want for any $x \in \mathcal{K}$, at least one "signal" from x to reach some Γ for $t < T$. Set

$$T_0(\mathcal{K}) = \max_{x \in \mathcal{K}} \operatorname{dist}(x, \Gamma).$$

The uniqueness condition then should be

$$T \geq T_0(\mathcal{K}). \qquad (*)$$

Theorem (Stefanov–U, IP 2011)

Let $c = 1$ outside Ω, and let $\partial\Omega$ be strictly convex. Then if $T \geq T_0(\mathcal{K})$, if $\Lambda f = 0$ on $[0, T] \times \Gamma$ and $\operatorname{supp} f \subset \mathcal{K}$, then $f = 0$.

Proof based on Tataru's uniqueness continuation results. Generalizes a similar result for constant speed by Finch, Patch and Rakesh.
As before, without (*), one can recover f on the reachable part of $\mathcal{K}$. Of course, one cannot recover anything outside it, by finite speed of propagation. Therefore,

(*) is an "if and only if" condition for uniqueness with partial data.

Stability

Heuristic arguments for stability: To be able to recover f from Λf on $[0, T] \times \Gamma$ *in a stable way*, we need to recover all singularities. In other words, we should require that

$\forall (x, \xi) \in \mathcal{K} \times S^{n-1}$, the ray (geodesic) through it reaches Γ at time $|t| < T$.

We show next that this is an "if and only if" condition (up to replacing an open set by a closed one) for stability. Actually, we show a bit more.

Proposition (Stefanov–U)

If the stability condition is not satisfied on $[0, T] \times \bar{\Gamma}$, *then there is no stability, in any Sobolev norms.*

A reformulation of the stability condition

- Every geodesic through $\mathcal{K}$ intersects Γ.
- $\forall (x, \xi) \in \mathcal{K} \times S^{n-1}$, the travel time along the geodesic through it satisfies $|t| < T$.

Let us call the least such time $T_1/2$, then $T > T_1/2$ as before.
In contrast, any small open Γ suffices for uniqueness.

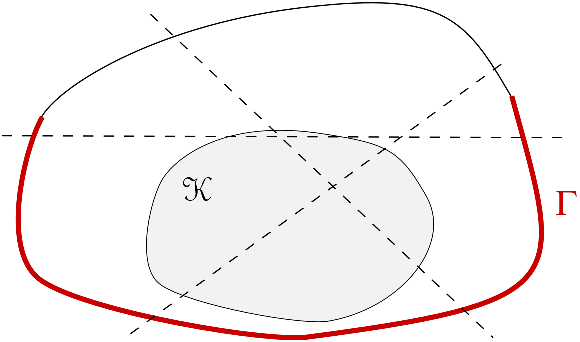

Let A be the "modified time reversal" operator as before. Actually, ϕ will be 0 because of χ below. Let $\chi \in C_0^\infty([0,T] \times \partial\Omega)$ be a cutoff (supported where we have data).

Theorem

$A\chi\Lambda$ is a zero order classical ΨDO in some neighborhood of $\mathcal{K}$ with principal symbol

$$\frac{1}{2}\chi(\gamma_{x,\xi}(\tau_+(x,\xi))) + \frac{1}{2}\chi(\gamma_{x,\xi}(\tau_-(x,\xi))).$$

If $[0,T] \times \Gamma$ satisfies the stability condition, and $|\chi| > 1/C > 0$ there, then
(a) $A\chi\Lambda$ is elliptic,
(b) $A\chi\Lambda$ is a Fredholm operator on $H_D(\mathcal{K})$,
(c) there exists a constant $C > 0$ so that

$$\|f\|_{H_D(\mathcal{K})} \le C\|\Lambda f\|_{H^1([0,T]\times\Gamma)}.$$

(b) follows by building a parametrix, and (c) follows from (b) and from the uniqueness result.
In particular, we get that for a fixed $T > T_1$, the classical Time Reversal is a parametrix (of infinite order, actually).

Reconstruction

One can constructively write the problem in the form

Reducing the problem to a Fredholm one

$$(I-K)f = BA\chi\Lambda f \quad \text{with the r.h.s. given,}$$

i.e., B is an explicit operator (a parametrix), where K is compact with 1 not an eigenvalue.

Constructing a parametrix without the ΨDO calculus.

Assume that the stability condition is satisfied in the interior of $\operatorname{supp}\chi$. Then

$$A\chi\Lambda f = (I-K)f,$$

where $I-K$ is an elliptic ΨDO with $0 \le \sigma_p(K) < 1$. Apply the formal Neumann series of $I-K$ (in Borel sense) to the l.h.s. to get

$$f = (I+K+K^2+\dots)A\chi\Lambda f \mod C^\infty.$$

Numerical Experiments: partial data

Zebras: non-trapping speed c_1, one-side missing

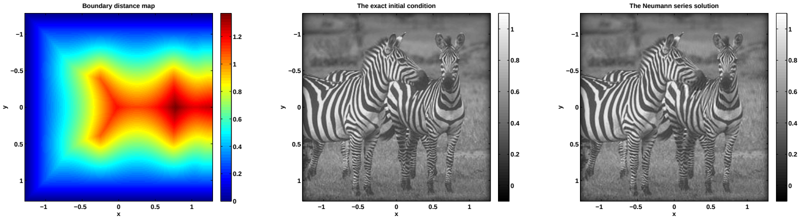

The boundary distance map | Exact | NS

Figure: non-trapping sound speed c_1, one-side missing, $T = 4.7$.

Zebras: non-trapping speed c_1, two-side missing

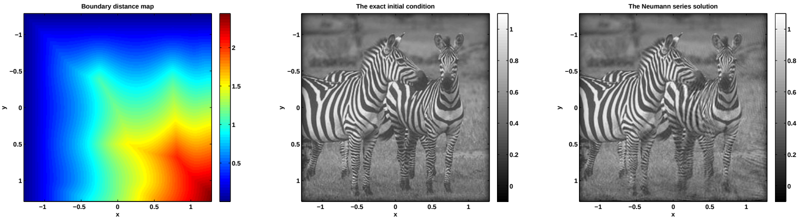

The boundary distance map　　　　Exact　　　　NS

Figure: non-trapping sound speed c_1, two-side missing, $T = 4.7$.

Modified zebras: non-trapping speed c_1, two-side missing

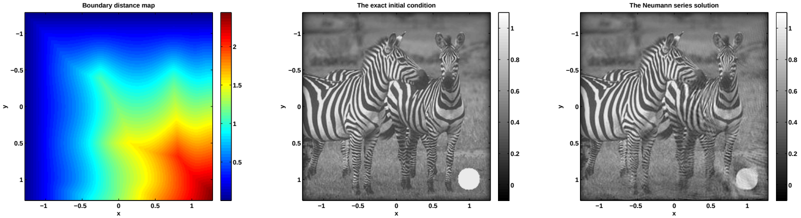

The boundary distance map Exact NS

Figure: non-trapping sound speed c_1, two-side missing, $T = 4.7$.

Zebras: trapping speed c_3, one-side missing

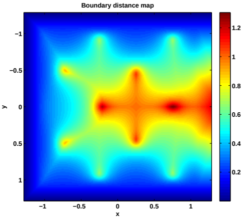

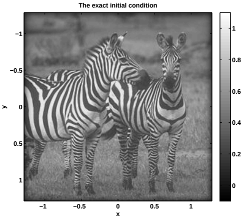

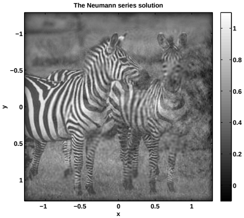

The boundary distance map | Exact | NS

Figure: trapping sound speed c_3, one-side missing, $T = 4.92$.

Zebras: trapping speed c_3, two-side missing

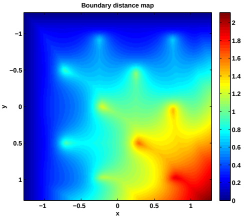

The boundary distance map

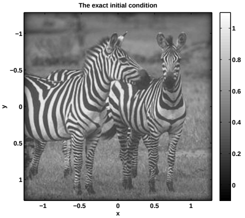

Exact

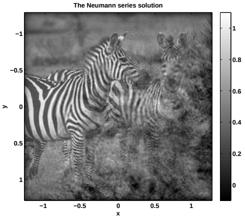

NS

Figure: trapping sound speed c_3, two-side missing, $T = 4.92$.

Examples: Non-trapping speed, 1 and 2 sides missing

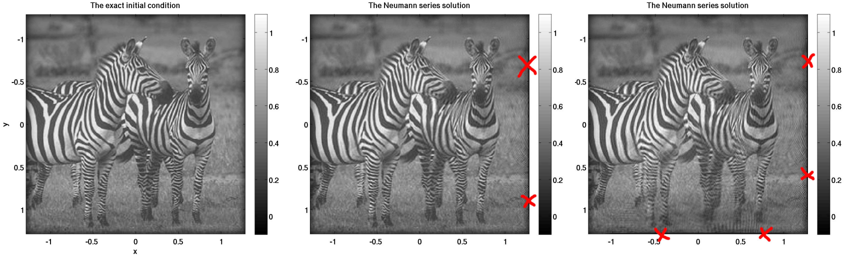

original NS, 3 sides, error $= 7.99\%$ NS, 2 sides, error $= 12.2\%$

Partial data reconstruction, non-trapping speed, $T = 4T_0$.

Determining the sound speed (Manohar et al, Appl. Phys. Lett. 2007)

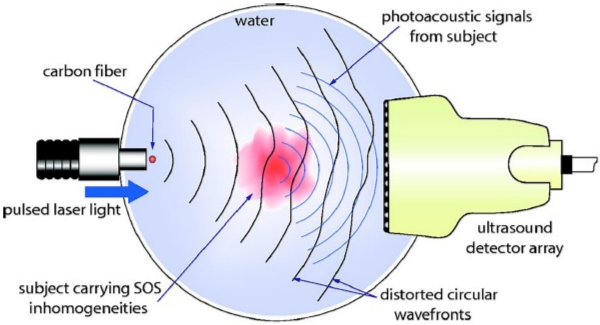

A schematic of the method to measure speed-of-sound cross-sectional images in a photo-acoustic imager. Ultrasound transients are generated in the absorbing carbon fiber placed in the path of light illuminating the sample. The time-of-arrival of the ultrasound transient is measured at each element of the ultrasound detector array. The photo-acoustic signals from the object can be measured as well.

2^{nd}-Step: Quantitative Photo-Acoustic Tomography (QPAT)

In the diffusive regime, **optical radiation** is modeled by:

$$-\nabla \cdot \gamma(x)\nabla u + \sigma(x)u = 0 \text{ in } X \qquad u = g \text{ on } \partial X \qquad \textbf{Illumination,}$$

$$H(x) = \Gamma(x)\sigma(x)u(x) \text{ in } X \qquad \textbf{Internal Functional.}$$

The **objectives** of *quantitative PAT* are to understand:

- What we can reconstruct of $(\gamma(x), \sigma(x), \Gamma(x))$ from knowledge of $H_j(x)$, $1 \leq j \leq J$ obtained for illuminations $g = g_j$, $1 \leq j \leq J$.
- How stable the reconstructions are.
- How to choose J and the illuminations g_j.

2^{nd}-Step: Quantitative Photo-Acoustic Tomography (QPAT)

In **Thermo-Acoustic Tomography**, low-frequency radiation is used.

Using a (scalar) **Helmholtz model** for radiation, **quantitative TAT** is

$$\Delta u + n(x)k^2 u + ik\sigma(x)u = 0 \text{ in } X, \qquad u = g \text{ on } \partial X \qquad \textbf{Illumination,}$$

$$H(x) = \sigma(x)|u|^2(x) \text{ in } X \qquad \textbf{Internal Functional}.$$

QTAT consists of uniquely and stably reconstructing $\sigma(x)$ from knowledge of $H(x)$ for appropriate illuminations g.

QPAT with two/more measurements

$$-\nabla\cdot\gamma(x)\nabla u+\sigma(x)u=0 \text{ in } X,\quad u=g \text{ on } \partial X,\quad H(x)=\Gamma(x)\sigma(x)u(x).$$

Let (g_1, g_2) providing (H_1, H_2). Define $\beta = H_1^2\nabla\frac{H_2}{H_1}$. **IF:** $|\beta|\geq c_0>0$, then

Theorem (Bal-U, IP 2010)

(i) (H_1, H_2) *uniquely determine the whole measurement operator* $g\in H^{\frac{1}{2}}(\partial X)\mapsto\mathcal{H}(g)=H\in H^1(X)$.
(ii) The measurement operator $\mathcal{H}$ *uniquely determines*

$$\chi(x):=\frac{\sqrt{\gamma}}{\Gamma\sigma}(x),\qquad q(x):=-\Big(\frac{\Delta\sqrt{\gamma}}{\sqrt{\gamma}}+\frac{\sigma}{\gamma}\Big)(x).$$

(iii) (χ, q) *uniquely determine* (H_1, H_2).

Two well-chosen measurements suffice to reconstruct (χ, q). Three or more measurements give no new information. (Bal-Ren, 2011)

Quantitative PAT

The proof of (i) & (ii) is based on the *elimination* of σ to get

$$-\nabla\cdot\chi^2\Big[H_1^2\nabla\frac{H}{H_1}\Big]=0 \text{ in } X \quad (\chi,H) \text{ known on } \partial X.$$

Then we verify that $q := -\Big(\frac{\Delta\sqrt{\gamma}}{\sqrt{\gamma}}+\frac{\sigma}{\gamma}\Big)(x) = -\frac{\Delta(\chi H_1)}{\chi H_1}$.

(iii) Finally, define $(\Delta+q)v_j=0$ to get $H_j=\frac{v_j}{\chi}$.

The **IF** implies that **vector field** $H_1^2\nabla\frac{u_2}{u_1}\neq 0$. This is a qualitative statement on the absence of critical points of elliptic solutions.

Stability of the reconstruction

Assuming **IF** satisfied, then the reconstruction of (e.g.) χ is **stable**.

CGO method. Analyzing the transport equation by the method of characteristics and using CGO solutions, we show that for appropriate illuminations (and for $k \geq 3$):

$$\|\chi - \tilde{\chi}\|_{C^{k-1}(X)} \leq C\|H - \tilde{H}\|_{(C^k(X))^2}.$$

Reconstruction of two discontinuous parameters

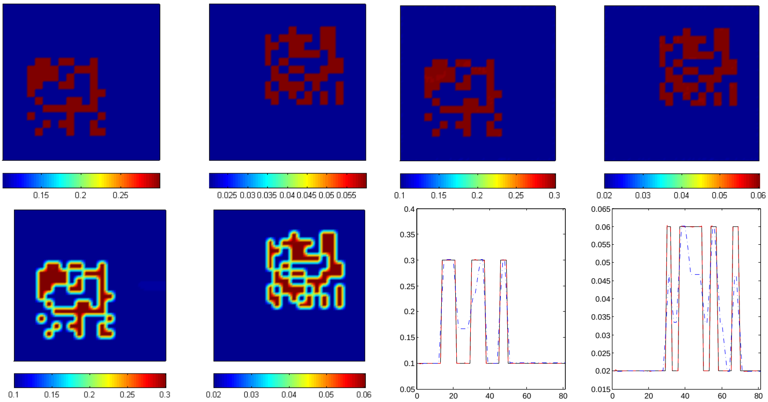

Stability result for QTAT

$$\Delta u + k^2 u + i\sigma(x) u = 0 \text{ in } X, \quad u = g \text{ on } \partial X, \quad H(x) = \sigma(x)|u|^2.$$

Theorem (Bal,Ren,U,Zhou'11)

Let σ and $\tilde{\sigma}$ be uniformly bounded functions in $Y = H^p(X)$ for $p > n$ with X the bounded support of the unknown conductivity.

Then there is an **open set of illuminations** g *such that*

$$H(x) = \tilde{H}(x) \text{ in } Y \qquad \text{implies that} \qquad \sigma(x) = \tilde{\sigma}(x) \text{ in } Y.$$

Moreover, there exists C such that $\boxed{\|\sigma - \tilde{\sigma}\|_Y \le C\|H - \tilde{H}\|_Y.}$

The **inverse scattering problem with internal data** is **well posed**. We apply a Banach fixed point **IF** appropriate functional is a contraction.

Discontinuous conductivity in TAT

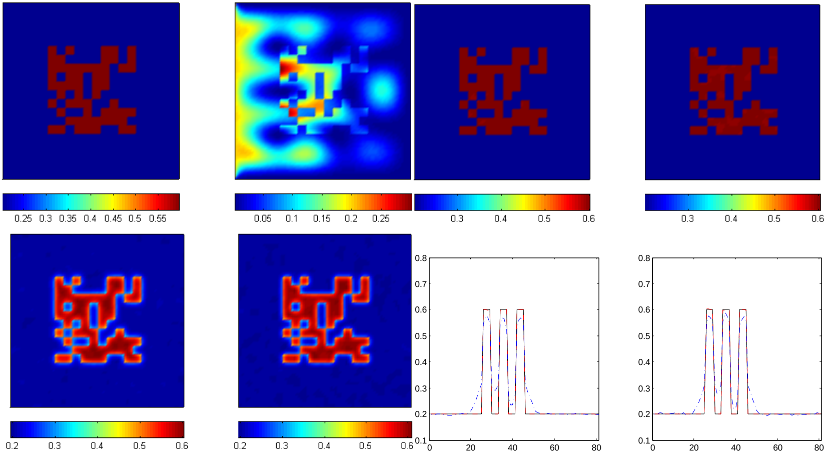

Vector fields and complex geometrical optics

- Take $\rho \in \mathbb{C}^n$ with $\rho \cdot \rho = 0$. Then $\Delta e^{\rho \cdot x} = 0$. For $u_j = e^{\rho_j \cdot x}$, $j = 1, 2$:

$$\Im\Big(e^{-(\rho_1+\rho_2)\cdot x} u_1^2 \nabla \frac{u_2}{u_1}\Big) = \Im(\rho_2 - \rho_1),$$

is a constant vector field $2k$ for $\rho_1 = k + ik^\perp$ and $\rho_2 = \bar{\rho}_1$.

- Let $u_\rho(x) = e^{\rho\cdot x}(1 + \psi_\rho(x))$ be a solution of $\Delta u_\rho + q u_\rho = 0$.

Theorem (Bal-U'10)

. *For q sufficiently smooth and $k \geq 0$, we have*

$$|\rho| \|\psi_\rho\|_{H^{\frac{n}{2}+k+\varepsilon}(X)} + \|\psi_\rho\|_{H^{\frac{n}{2}+k+1+\varepsilon}(X)} \leq C\|q\|_{H^{\frac{n}{2}+k+\varepsilon}(X)}.$$

- For **illuminations** g on ∂X close to *traces of* **CGO** *solutions* constructed in $\mathbb{R}^d$, we obtain "nice" vector fields $|\beta| \geq c_0 > 0$ and thus an open set of illuminations g for which stable reconstructions are guaranteed.

The IFs and the CGOs

Several HIPs require to verify qualitative properties of elliptic solutions:

- the absence of critical points in QPAT
- the contraction of appropriate functionals in QTAT

The existence of open sets of **illuminations** g_j such that these properties hold is obtained by means of **CGO** solutions.

Reconstructions from multiple solution measurements

Consider a *general scalar elliptic* equation

$$\nabla \cdot a \nabla u + b \cdot \nabla u + cu = 0 \quad \text{in } X, \qquad u = f \quad \text{on } \partial X$$

with a, b, c, $\nabla \cdot a$ of class $C^{0,\alpha}(\bar{X})$ for $\alpha > 0$, complex-valued, and $\alpha_0 |\xi|^2 \leq \xi \cdot (\Re a)\xi \leq \alpha_0^{-1} |\xi|^2$. For $\tau > 0$ a function on X, define

$$a_\tau = \tau a, \quad b_\tau = \tau b - a \nabla \tau, \quad c_\tau = \tau c$$

and the equivalence class $\mathfrak{c} := (a, b, c) \sim (a_\tau, b_\tau, c_\tau)$.

Let $I \in \mathbb{N}^*$ and $f_i \in H^{\frac{1}{2}}(\partial X)$ for $1 \leq i \leq I$ be I boundary conditions. Define $\mathfrak{f} = (f_1, \ldots, f_I)$. The measurement operator $\mathfrak{M}_{\mathfrak{f}}$ is

$$\mathfrak{M}_{\mathfrak{f}} : \mathfrak{c} \mapsto \mathfrak{M}_{\mathfrak{f}}(\mathfrak{c}) = (u_1, \ldots, u_I),$$

with u_j solution of the above elliptic problem with $f = f_j$.

Unique reconstruction up to gauge transformation

$$\nabla\cdot a\nabla u_j + b\cdot\nabla u_j + cu_j = 0 \quad \text{in } X, \qquad u_j = f_j \quad \text{on } \partial X, \quad 1\leq j\leq I.$$

Theorem (Bal-U 2012)

. Let $\mathfrak{c}$ and $\tilde{\mathfrak{c}}$ be two classes of coefficients with (a,b,c) and $\nabla\cdot a$ of class $C^{m,\alpha}(\bar X)$ for $\alpha>0$ and $m=0$ or $m=1$. We assume that the above elliptic equation is well posed for $\mathfrak{c}=(a,b,c)$.

Then for I sufficiently large *and for an* open set of boundary conditions $\mathfrak{f}=(f_j)_{1\leq j\leq I}$*, then $\mathfrak{M}_{\mathfrak{f}}(\mathfrak{c})$ uniquely determines $\mathfrak{c}$. Moreover, we have the following stability estimate*

$$\begin{aligned}\|(a,b+\nabla\cdot a,c)-(\tilde a,\tilde b+\nabla\cdot\tilde a,\tilde c)\|_{W^{m,\infty}(X)} &\leq C\|\mathfrak{M}_{\mathfrak{f}}(\mathfrak{c})-\mathfrak{M}_{\mathfrak{f}}(\tilde{\mathfrak{c}})\|_{W^{m+2,\infty}(X)},\\ \|b-\tilde b\|_{L^\infty(X)} &\leq C\|\mathfrak{M}_{\mathfrak{f}}(\mathfrak{c})-\mathfrak{M}_{\mathfrak{f}}(\tilde{\mathfrak{c}})\|_{W^{3,\infty}(X)},\end{aligned}$$

for $m=0,1$ and for an appropriate $(\tilde a,\tilde b,\tilde c)$ of $\tilde{\mathfrak{c}}$.

In several settings (typically when CGO solutions are available), we can choose $I=I_n=\frac{1}{2}n(n+3)$ with n spatial dimension and with I_n the dimension of $\mathfrak{c}$.

Unique reconstruction of the gauge

In some situations (such as the practical settings of QPAT and TE/MRE), the gauge in $\mathfrak{c}$ can be uniquely and stably determined:

Corollary (Bal-U 2012)

Under the hypotheses of the preceding theorem, and in the setting where $b = 0$, then $\mathfrak{M}_{\mathfrak{f}}(\mathfrak{c})$ uniquely determines $(\gamma, 0, c)$. Let us define $\gamma = \tau M^0$ where M^0 has determinant 1. Then we have the following stability result:

$$\|\tau - \tilde{\tau}\|_{W^{1,\infty}(X)} + \|(M^0, c) - (\tilde{M}^0, \tilde{c})\|_{L^\infty(X)} \leq C\|\mathfrak{M}_{\mathfrak{f}}(\mathfrak{c}) - \mathfrak{M}_{\mathfrak{f}}(\tilde{\mathfrak{c}})\|_{W^{2,\infty}(X)}.$$

From the practical point of view, the reconstruction of the determinant of γ is *more stable* than the reconstruction of the anisotropy of the (possibly complex valued) tensor γ. This has been observed numerically in a different setting.

Acousto-Electric Tomography (AET, also called UM-EIT)

- Scanning with ultrasound

- Ultrasound waves change conductivity

- This change is small but can be detected by electrical measurements on the boundary [Zhang,Wang 2004]

- This additional information solves ill-posedness of diffusion equation.

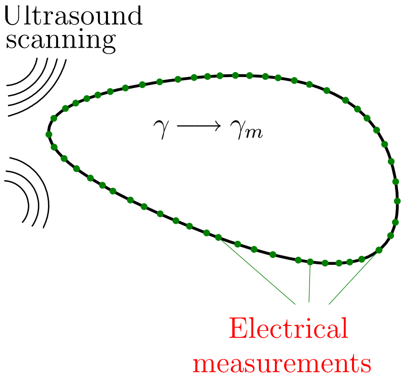

[Ammari, Bonnetier, Capdeboscq, Tanter and Fink 2008], [Kuchment, Kunyansky 2010, 2011], [Capdeboscq, Fehrenbach, de Gournay and Kavian 2009], [Bal 2011], [Bal, Bonnetier, Monard and Triki 2011], [Bal, Monard 2012], [Kocyigit, 2012], ...

Inverse Problem of AET

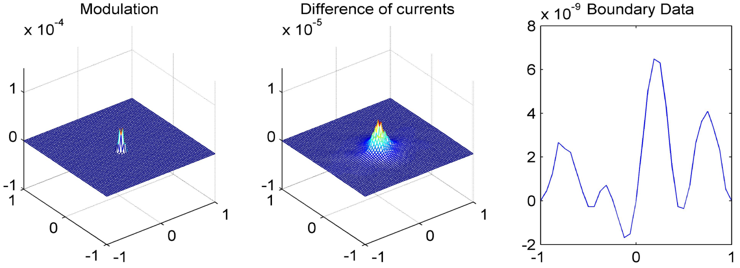

Conductivity after the ultrasound modulation $m \in C^\infty(\Omega)$ is modeled by

$$\gamma_m(x) = (1 + m(x))\gamma(x)$$

For any fixed potential $f \in H^{1/2}(\partial\Omega)$ boundary measurements are

$$M_f(m) := (\Lambda_{\gamma_m} - \Lambda_\gamma)f.$$

$\boxed{\text{Recover } \gamma \text{ from the knowledge of } M_f.}$

AET : Uniqueness

(Kocyigit, 2012) Uniqueness for one fixed boundary potential $f \in H^{1/2}(\partial\Omega)$.

$$M_f \xrightarrow[\text{1}^{\text{st}}\text{step}]{\text{using CGOs}} \sqrt{\gamma}\nabla u \xrightarrow[\text{2}^{\text{nd}}\text{step}]{} \gamma$$

1st step	2nd step
Uniqueness no conditions on f	**Uniqueness** if $\Lambda_\gamma f$ doesnot vanish on some small part of $\partial\Omega$ specified by [Kenig, Sjöstrand, Uhlmann 04]
	Lipschitz stable if $\|F(x)\|^{-1} \in L^2(\Omega)$

Use of CGO solutions

$$\langle M_f(m), g\rangle = \int_\Omega \gamma(\nabla u_m - \nabla u) \cdot \nabla G \, \mathrm{d}x + \int_\Omega m\gamma\nabla u_m \cdot \nabla G \, \mathrm{d}x$$

where <u>G is a CGO</u> solution. Set modulation to :

$$m(x) = e^{(-\rho - ik)\cdot x}$$ (complex modulation is defined by a "linearization")

$\Longrightarrow$ Recover $\int_\Omega e^{-ik\cdot x}\mu\nabla u \cdot \hat{\rho} \, \mathrm{d}x + O\left(\frac{1}{|\rho|}\right)$

AET : Inversion

(Kocyigit, 2012) Stable Inversion (one fixed boundary potential f)

1st step: Recovery of the current density J by an iterative algorithm

$$M_f \xrightarrow[\text{1st step}]{\hspace{6em}} J = \gamma \nabla u \xrightarrow[\text{2nd step (same as above)}]{\hspace{8em}} \gamma$$

Suppose ultrasound modulation m_z is focused about $z \in \Omega$ in $B_\varepsilon(z)$

$$\underbrace{\left(\sum_{i=1}^{n} \varepsilon^{-1} \langle M_f(m_z), x_i \rangle e_i \right)}_{\text{Known}} = I + R[\gamma] + O(\varepsilon)$$

where R is the matrix valued operator $(R[\gamma])_{j,i} := \langle \Lambda_\gamma(r_i|_{\partial\Omega}), x_j \rangle$,

$$\begin{aligned} \Delta w_i &= -(\nabla m_z)_i, & w_i\,|_{\partial\Omega} = 0 \quad &\text{on } \partial\Omega \\ \nabla \cdot (\gamma \nabla r_i) &= \nabla \cdot (w_i \gamma^{-1} \nabla \gamma), & \partial_\nu r_i = 0 \quad &\text{on } \partial\Omega. \end{aligned}$$

- Algorithm converges when $\gamma^{-1}\nabla\gamma$ is small in $L^2(\Omega)$
- Complexity $O(N)$, N is the mesh size (i.e. locations of ultrasound focus)

AET : Numerical Simulations

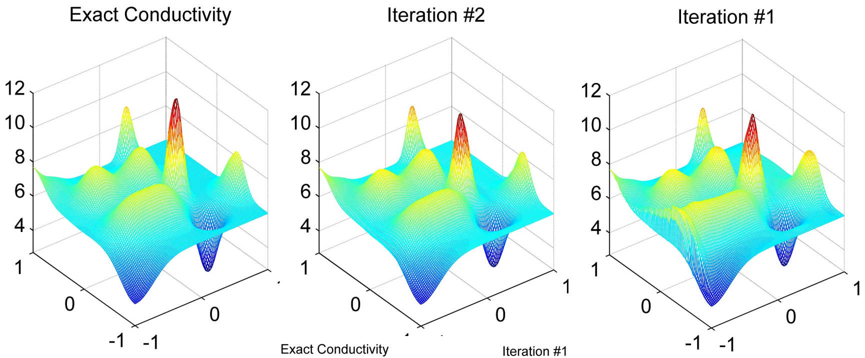

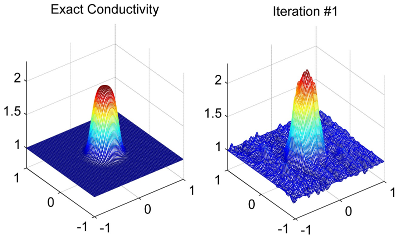

The noise level of %20 is introduced to the measurement data.

Electro-seismic effect

When a porous rock is saturated with an electrolyte, electrical field and seismic waves are coupled through the phenomenon of electro-kinetics. The governing macroscopic models of the electro-seismic effect were derived by Pride(1994),

$$\boxed{\begin{aligned} \nabla \times E &= i\omega\mu H, \\ \nabla \times H &= (\sigma - i\epsilon\omega)E + L(-\nabla p + \omega^2 \rho_f u) + j_s, \end{aligned}}$$

Maxwell equations

$$\boxed{\begin{aligned} -\omega^2(\rho u + \rho_f w) &= \nabla \cdot \tau, \\ -i\omega w &= LE + \tfrac{\kappa}{\eta}(-\nabla p + \omega^s \rho_f u), \\ \tau &= (\lambda \nabla \cdot u + c\nabla \cdot w)I + G(\nabla u + \nabla u^T), \\ -p &= c\nabla \cdot u + M\nabla \cdot w, \end{aligned}}$$

Biot's equations

Inverse problem of electro-seismic effect

The inverse problem of the electro-seismic effect consists of two steps.

- The first step is to invert Biot's system and recover the internal coupling term $\boxed{d := LE}$ from boundary measurements. We assume this step is done and mainly focus on the second step.
- By assuming the coupling effect is weak, multiple coupling can be neglected and the coupling system is linearized. The second step of the inverse problem is to invert Maxwell equations

$$\boxed{\begin{aligned}\nabla \times E &= i\omega\mu H,\\ \nabla \times H &= (\sigma - i\epsilon\omega)E + j_s\end{aligned}}$$

  and recover the medium conductivity $\boxed{\sigma}$ and the coupling coefficient $\boxed{L}$ from the boundary measurements and the internal coupling data $\boxed{d = LE}$ from the first step.

Uniqueness result

Theorem (J. Chen and Y. Yang, 2012)

Let Ω be an open, bounded, connected domain in $\mathbb{R}^3$ with C^k boundary $\partial\Omega$. Assume that (L, σ) and $(\tilde{L}, \tilde{\sigma})$ are two elements in $C^{k+1}(\bar{\Omega}) \times H^{\frac{3}{2}+3+d+\epsilon}(\Omega)$ with $L|_{\partial\Omega} = \tilde{L}|_{\partial\Omega}$. Let $D = (d_j)$ and $\tilde{D} = (\tilde{d}_j)$, $j = 1, \ldots, 4$, be the internal data for coefficients (L, σ) and $(\tilde{L}, \tilde{\sigma})$, respectively, and with boundary conditions $G = (g_j)$, $j = 1, \ldots, 4$.

Then there is a set of illuminations $G \in (C^{k+4}(\partial\Omega))^2$, such that if $\boxed{D = \tilde{D}}$, then $\boxed{(L, \sigma) = (\tilde{L}, \tilde{\sigma})}$ in Ω.

Sketch of the proof

Colton & Päivärinta (1992) constructed CGO solutions to Maxwell equation

$$\boxed{\nabla \times \nabla \times E - k^2 nE = 0}$$

of the form

$$\boxed{E(x) = e^{i\zeta\cdot x}(\eta + R_\zeta(x)).}$$

Let E_1, E_2 be two solutions to the Maxwell equation. We have that

$$\boxed{E_2 \cdot \nabla \times \nabla \times E_1 - E_1 \cdot \nabla \times \nabla \times E_2 = 0.}$$

By substituting $E_j = d_j/L$, we have a transport equation

$$\boxed{\beta \cdot \nabla L + \gamma L = 0.}$$

When the boundary illuminations are chosen to be close to the boundary values of CGO solutions, we can prove that, for a constant ζ_0,

$$\boxed{\|\beta - 4L^2\zeta_0\|_{C^k(\Omega)} = O(1/|\zeta|),}$$

Thus the transport equation admits a unique solution.

Stability result

To consider the stability of the reconstruction, additional geometric information of $\partial\Omega$ is needed.

Hypothesis

let Ω be an open, bounded, connected domain in $\mathbb{R}^3$. There exists $R < \infty$ such that for each $y \in \partial\Omega$, we have $\Omega \subseteq B_y(R)$, where $B_y(R)$ is a ball of radius R that is tangent to $\partial\Omega$ at y.

Theorem (J. Chen and Y. Yang, 2012)

let $k \geq 3$. Let Ω satisfies the above hypothesis. Assume that (L, σ) and $(\tilde{L}, \tilde{\sigma})$ are two elements in $C^{k+1}(\bar{\Omega}) \times H^{\frac{3}{2}+3+k+\epsilon}(\Omega)$ with $L|_{\partial\Omega} = \tilde{L}|_{\partial\Omega}$. Let $D = (d_j)$ and $\tilde{D} = (\tilde{d}_j)$, $j = 1, \ldots, 4$, be the internal data for coefficients (L, σ) and $(\tilde{L}, \tilde{\sigma})$, respectively, and with boundary conditions $G = (g_j)$, $j = 1, \ldots, 4$.
Then there is a set of illuminations $G \in (C^{k+4}(\partial\Omega))^4$, such that

$$\boxed{\|L - \tilde{L}\|_{C^{k-1}(\Omega)} + \|\sigma - \tilde{\sigma}\|_{C^{k-2}(\Omega)} \leq C\|D - \tilde{D}\|_{C^{k+1}(\Omega)^4}.}$$